Proceeding of the 38th Society of Vacuum Coaters Meeting, 425-431 (1995).
R.W. Knoll, and J. A. Theil

Effects of Process Parameters on PECVD Silicon Oxide and Aluminum Oxide Barrier Films

R.W. Knoll and J.A. Theil, Johnson Controls, Inc., Milwaukee, WI

Keywords: PECVD Oxide films
Permeation barrier films

ABSTRACT

Silicon oxide based barrier films from organosilicon precursors have been deposited on PET film in a lab-scale coater using plasma-enhanced chemical vapor deposition (PECVD) . Exploratory work on aluminum oxide films from a trimethylaluminum (TMA) precursor, as well as mixed silica alumina films is also reported. Deposition experiments were performed in a cylindrical coater containing a central axial RF electrode with gas flow in the axial direction. Coatings were deposited on 2 mil PET films in contact with the central electrode. The primary objective was to map out, using designed experiments, the behavior of SiO_x - based film properties over a range of process parameter settings. Factors studied were rf power, precursor concentration, gas velocity and gas pressure. Oxygen permeation rates of coated PET films were measured in a Mocon analyzer. Film deposition rate and index, compositional characteristics as measured by FTIR analysis, and thickness uniformity along the electrode axis, will also be described. Film permeability and deposition rate varied by more than an order of magnitude over the range of process variables tested. The TMA precursor was found to be more reactive than an organosilicon precursor such as HMDSO, and had a greater tendency for non uniform film deposition.

INTRODUCTION

Transparent oxide barrier films for reducing gas and water vapor permeation through plastic packaging materials are of commercial interest for various food and beverage applications. Numerous papers have described physical vapor deposition (PVD) and plasma-enhanced chemical vapor deposition (PECVD) processes for low temperature deposition of oxide barrier films, primarily on plastic web [1-4]. However, few systematic studies of low temperature PECVD process behavior have been published. This paper presents an experimental study of plasma-enhanced deposition of SiO_x thin films from hexamethyldisiloxane (HMDSO) precursor. The framework for this study is a four-factor statistically designed experiment of the central composite type. Some exploratory work on AlO_x deposition from trimethylaluminum (TMA) precursors is also reported. The experiments were performed in a lab scale reactor having a simple cylindrical tube geometry to allow control of gas flow and plasma distribution. The main purpose of this work was to determine how local process conditions affect film growth characteristics and oxygen barrier effectiveness. A related paper in this conference [5] describes some mechanical properties of SiO_x films produced by the same process.

EXPERIMENTAL

Coater and Process Description The cylindrical PECVD tube coater is shown schematically in Fig. 1. It consists of a 6.25 in (16 cm) ID by 18 in (46 cm) long, thick-walled glass tube surrounding a central RF electrode assembly. The glass tube serves as the vacuum chamber. It is capped by a stainless steel flange containing

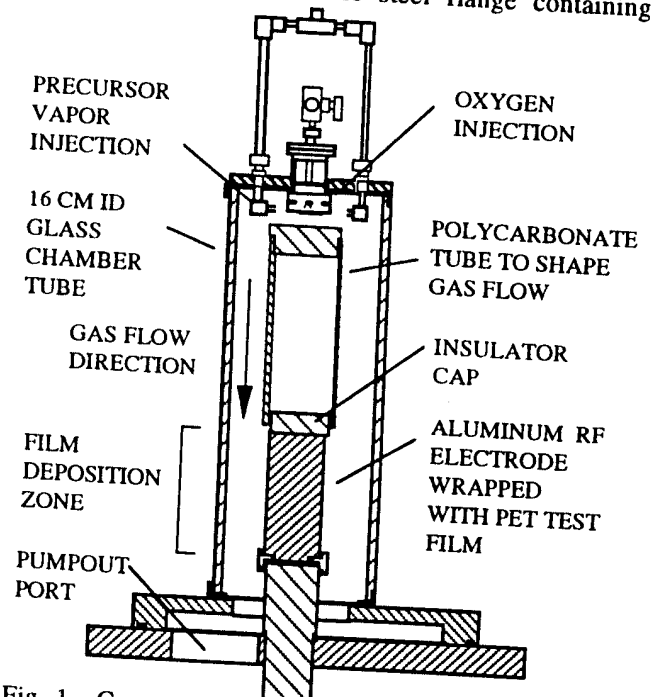

Fig. 1. Cross sectional diagram of cylindrical vacuum chamber for PECVD on PET sheet samples.

the O_2 and precursor vapor injectors. The electrode is a 2.5 in (6.4 cm) OD by 5.5 in (14 cm) polished aluminum cylinder capped by Delrin insulator disks to constrain the

38th Annual Technical Conference Proceedings (1995) ISSN 0737-5921

Table I. Experimental Design and Summary of Results for SiOx Central Composite Experiment.

Std Ord	Pat-tern	HMDSO Conc. 1E-10 moles/cc	Average Gas Velc. cm/sec	Pres-sure mTorr	RF Power Density W/cm2	Flow Rates O2 sccm	Flow Rates HMDS sccm	Depos. Rate (Avg) Å/min	Uniformity Factor	Refrac. Index (Avg)	Si-O-Si Wave-number cm-1	Prcsr Area / Thk	Msrd O2 Prm Rate per 1000Å cc/m2day
1	----	1.2	100	150	0.30	195	3.0	1278	0.901	1.436	1055.6	0.0000	1.0
2	---+	1.2	100	150	0.70	195	3.0	1040	0.654	1.442	1056.1	0.0000	4.2
3	--+-	1.2	100	350	0.30	458	3.0	1016	0.764	1.460	1058.7	0.0000	6.0
4	--++	1.2	100	350	0.70	458	3.0	803	0.474	1.452	1058.4	0.0000	26.9
5	-+--	1.2	200	150	0.30	390	5.9	1533	0.943	1.469	1054.6	0.0000	1.7
6	-+-+	1.2	200	150	0.70	390	5.9	1859	0.901	1.462	1054.5	0.0000	2.1
7	-++-	1.2	200	350	0.30	917	5.9	1515	0.903	1.463	1062.3	0.0000	4.3
8	-+++	1.2	200	350	0.70	917	5.9	1704	0.750	1.466	1057.8	0.0000	9.9
9	+---	3.0	100	150	0.30	190	7.4	2194	0.978	1.481	1048.4	0.0107	8.7
10	+--+	3.0	100	150	0.70	190	7.4	2599	0.901	1.473	1051.0	0.0000	3.9
11	+-+-	3.0	100	350	0.30	454	7.4	2401	0.914	1.462	1054.8	0.0209	21.1
12	+-++	3.0	100	350	0.70	454	7.4	2707	0.766	1.456	1061.7	0.0000	15.7
13	++--	3.0	200	150	0.30	381	14.8	2499	0.939	1.485	1045.8	0.0127	12.8
14	+++-	3.0	200	150	0.70	381	14.8	3488	0.968	1.474	1047.0	0.0021	7.4
15	+++-	3.0	200	350	0.30	908	14.8	2664	0.925	1.462	1051.2	0.0348	26.8
16	++++	3.0	200	350	0.70	908	14.8	3938	0.888	1.450	1057.6	0.0118	25.7
17	-ooo	0.3	150	250	0.50	493	1.1	328	0.496	1.466	1059.0	0.0000	30.0
18	+ooo	3.9	150	250	0.50	480	14.5	3889	0.917	1.458	1050.8	0.0118	26.4
19	o-oo	2.1	50	250	0.50	162	2.6	825	0.513	1.441	1058.5	0.0000	19.6
20	o+oo	2.1	250	250	0.50	811	13.0	2955	0.915	1.460	1056.6	0.0000	9.4
21	oo-o	2.1	150	50	0.50	91	7.8	1695	0.926	1.498	1040.3	0.0000	1.0
22	oo+o	2.1	150	450	0.50	882	7.8	2108	0.870	1.460	1062.0	0.0031	5.4
23	ooo-	2.1	150	250	0.10	487	7.8	1176	0.945	1.466	1051.1	0.0233	25.9
24	ooo+	2.1	150	250	0.90	487	7.8	2701	0.813	1.460	1056.3	0.0000	3.1
25	oooo	2.1	150	250	0.50	487	7.8	2480	0.914	1.465	1057.7	0.0000	9.7
26	oooo	2.1	150	250	0.50	487	7.8	2606	0.927	1.463	1058.7	0.0000	6.6
27	oooo	2.1	150	250	0.50	487	7.8	2503	0.917	1.463	1057.2	0.0000	4.8
28	oooo	2.1	150	250	0.50	487	7.8	2447	0.891	1.461	1057.8	0.0012	4.6
29	oooo	2.1	150	250	0.50	487	7.8	2587	0.899	1.464	1057.8	0.0000	5.6
30	oooo	2.1	150	250	0.50	487	7.8	2668	0.892	1.464	1058.4	0.0033	10.2
31	oooo	2.1	150	250	0.50	487	7.8	2467	0.903	1.464	1058.0	0.0000	

discharge to the cylindrical surface. The plastic film to be coated is wrapped snugly around the electrode. A polycarbonate spacer tube positioned above the electrode provides an annulus of nearly constant cross section (~167 cm^2) along the length of the chamber. Reactant gases injected at the top mix as they flow through the chamber and are pumped through an annular port surrounding the electrode base.

RF power from an ENI Plasmaloc 2HF power supply, at a frequency of 250 KHz, is applied to the electrode via an Astech Model ATK-100 RF matching network. RF power is monitored using a Bird Model 4411 RF wattmeter. Reactant gas flow rates and chamber pressure are controlled by an MKS feedback control system. HMDSO vapor flow is controlled by an MKS Model 1150C vapor mass flow controller. TMA vapor flow rate is controlled by a needle valve. Flow rate was estimated to ± 20% from pressure rate-of-rise measurements, compared with known HMDSO flow rate vs. rate-of-rise curves.

For all work reported here, the substrate film was 2 mil (51 µm) thick Dupont Mylar PET type A (untreated, biaxially oriented). Barrier film deposition was at approximately room temperature, as the solid aluminum electrode acted as a heat sink for the PET film. Small silicon witness samples (~1.5 cm x 1 cm), cut from double side polished <100> Si wafers, were attached to the PET substrate at various positions on the electrode. These were used for SiO_x film property measurements.

Design of Experiment Response surface methodology [6] employing a four-factor central composite experimental design was used to characterize the SiO_x deposition process. This design consists of 31 runs: a full factorial (runs 1-16) with star points (runs 17-24) and repeated centerpoint (runs 25-31) as listed in Table I. Process factors (variables) tested were precursor concentration (1E-10 moles/cc), average gas velocity or "plug" velocity (cm/sec,), pressure (mTorr), and RF power density (W/cm^2). Average gas velocity is the volumetric gas flow rate divided by cross sectional area.

Precursor concentration was calculated from the ideal gas law. The area of exposed electrode was ~ 205 cm^2, so a power density of 0.5 W/cm^2 required ~ 103 W of load power. All of the factor settings, as well as actual O_2 and HMDSO gas flow rates for each run, are listed in Table I. These settings span most of the practical operating range of the reactor system. For each response measured, the data were analyzed and fit to a second degree polynomial using the statistical visualization software package JMP [7].

Thin Film Characterization Film thickness and index of refraction were measured using an automated Gaertner Model L116A ellipsometer, while chemical characteristics were obtained by FTIR (Fourier transform infrared) transmission spectroscopy using a Bomem Model MB155 spectrometer. Because of experimental difficulties in measuring characteristics of thin films on PET substrates, the ellipsometry and FTIR measurements were performed on films deposited on the Si witness samples mentioned earlier.

O_2 Permeation Measurements Oxygen permeation transmission rates (O_2TR) of barrier coated 2 mil PET film samples were measured using MOCON (Modern Controls, Inc.) instruments. Most measurements were performed on a MOCON Oxtran Basic (50 cm^2 test area) at 23°C, under wet O_2 conditions. PET films intended for O_2 permeation test had one witness sample attached (at 7 cm level, out of the test region) to confirm SiO_x film thickness.

RESULTS AND DISCUSSION

SiO_x Film Compositional Characteristics The Fourier transform infrared (FTIR) spectrum over the range 4000 cm^{-1} to 400 cm^{-1} was obtained and analyzed for SiO_x films from each run of the central composite experiment (on Si witness samples from the 3 cm and 7 cm positions). All of the films shared basic spectral characteristics, the most prominent being the large Si-O-Si stretch peak that lies at 1075 cm^{-1} for thermal SiO_2. The Si-O-Si stretch peak for these films ranged from 1062 to 1040 cm^{-1}, as listed in Table I. Also evident were: a broad OH peak at 3650 ~ 3350 cm^{-1}; a small, broad C=O peak at 1730 ~ 1690 cm^{-1}; and in some cases, a small Si-CH_3 at 1275 ~ 1260 cm^{-1} from residual precursor. FTIR characteristics of similar SiO_x films have been previously described in detail by Theil, et al [8]. The normalized areas (peak area/film thickness) for each of the above four peaks were treated as responses and were fit to second degree polynomial models using the JMP [7] software. Both the Si-O-Si and Si-CH_3 normalized areas could be fit well. The Si-O-Si wavenumber also fit well, i.e., it responded in an orderly manner to changes in the process settings. The JMP model fit showed that HMDSO concentration and process pressure strongly affected the peak wavenumber, although in opposing directions. Gas velocity and power density effects were relatively weak. Correlation of FTIR features with O_2 permeation rates will be discussed in future paper.

Refractive Index The average index of refraction (averaged from the 3, 7, and 11 cm witness sample positions) for each run is also listed in Table I. Index ranged from 1.436 (Run 1) to 1.498 (Run 21), compared with 1.467 for thermal SiO_2. Statistical analysis showed a moderate positive effect of HMDSO concentration on index, and a moderate negative effect of pressure.

SiO_x Film Deposition Rate and Uniformity The average SiO_x deposition rate (R_{av}) for each run condition is listed in Table I. R_{av} was obtained from film thickness measurements at the 3, 7, and 11 cm positions on the electrode. A uniformity factor defined as

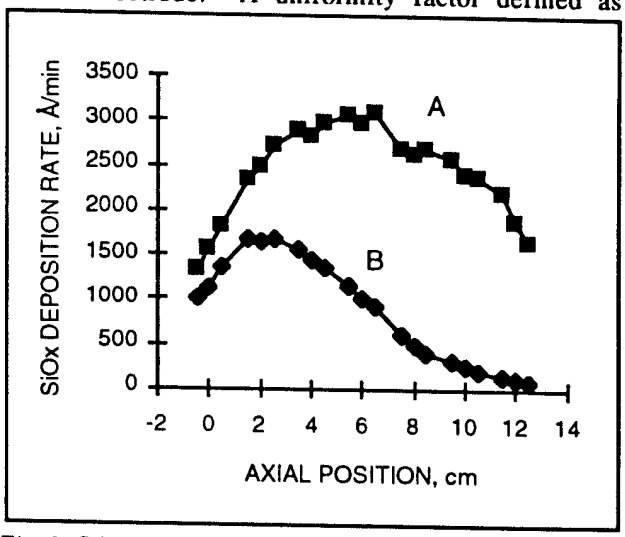

Fig. 2 Silicon oxide film deposition-rate axial profiles for two different experimental conditions: A: (center point conditions) 250 mTorr, 0.5 W/cm², 2.1 E-10 moles/cc HMDSO, 150 cm/sec gas velocity. B: Same as above except 50 cm/sec gas velocity.

R_{av} /R_{max} , where R_{max} is the maximum deposition rate is listed in the next column. R_{av} varies by an order of magnitude, from 328 Å/min for the low-HMDSO starpoint of Run #17, to 3,938 Å/min for Run #16. R_{av} for the seven centerpoint runs is 2,537 Å/min ± 83.4 Å/min.

Axial SiO_x film deposition-rate profiles for the centerpoint deposition condition (A) and for a lower gas-velocity condition (B) are plotted in Fig. 2. The top (upstream) end of the electrode lies at the 0 cm position. For both cases, deposition rate rises rapidly as the reactant gases encounter the plasma zone. For (A), the profile is quite symmetric, with a peak rate of nearly 3,000 Å/min. The decline in deposition rate beyond midplane is attributed to both a decrease in the plasma density and to

HMDSO depletion in the reactant gas mixture as the gases flow downstream. For the lower gas-velocity case (B), R_{max} is much lower than for (A), and it occurs farther upstream.

The contour plot presented in Figs. 3a shows how the average SiO_x deposition-rate responds to changes in HMDSO concentration and power density, at a pressure of 250 mTorr and gas velocity of 150 cm/sec. This plot was calculated from the second degree polynomial fit generated by the JMP [7] software. This behavior is typical of other pressure and velocity settings also. Generally, at a fixed power density, R_{av} increases almost linearly with HMDSO concentration. At fixed HMDSO concentration, R_{av} first increases then reaches a maximum and falls off

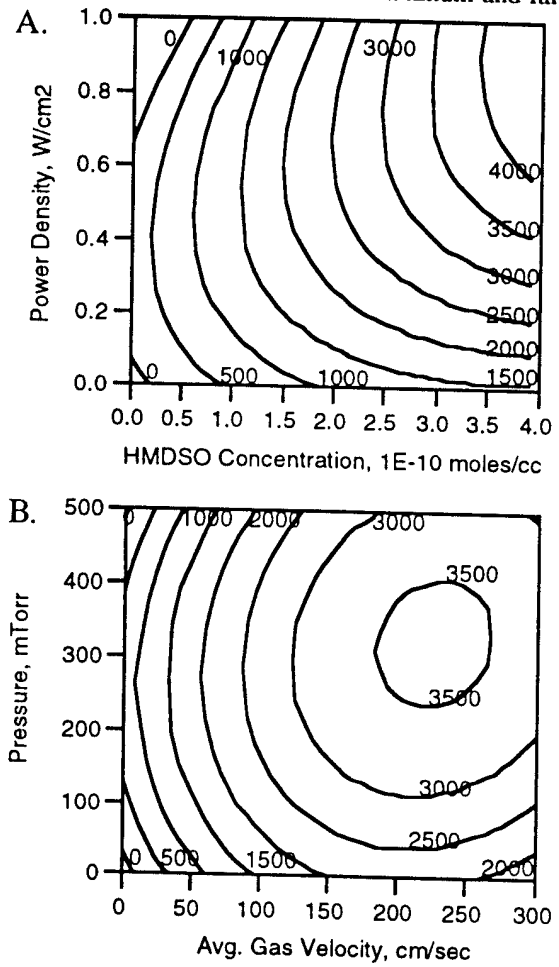

Fig. 3. Contour plots of the average SiO_x deposition rate (Å/min), as a function of A: HMDSO concentration and RF power density at 250 mTorr and gas velocity of 150 cm/sec. B: gas velocity and pressure, at power density of 0.5 W/cm2 and HMDSO concentration of 3.0E-10 moles/cc. Both plots are typical of the deposition rate behavior over most of the experimental range studied. They were generated from a second degree polynomial fit to the data. Rsq =0.967 for this fit.

with increasing power. The model predicts that R_{av} continues to rise with both increasing power density *and* HMDSO concentration. Fig. 3b shows an example of the effect of pressure and average gas velocity on R_{av}, in this case at 0.5 W/cm^2 and 3.0 E-10 moles/cc HMDSO. R_{av} reaches a maximum at ~ 350 mTorr and 240 cm/sec gas velocity. Again, this behavior is typical of that seen over most of the factor settings examined here.

Examples of the effects of deposition parameters on SiO_x

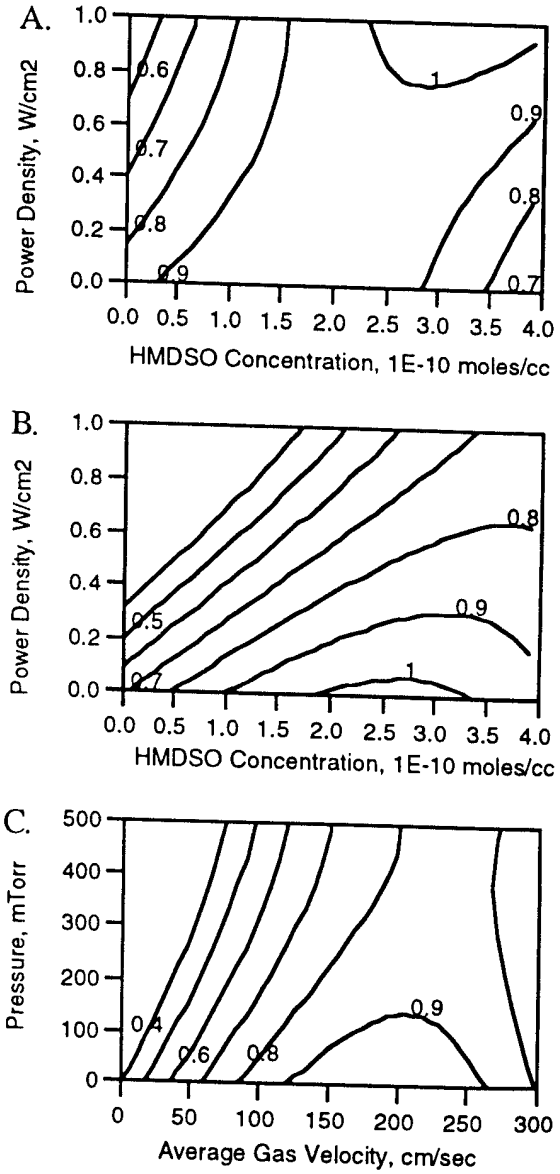

Fig. 4. Contour plots of the SiO_x film thickness uniformity factor as a function of HMDSO concentration and RF power density, at two conditions of pressure and gas velocity: A) 150 mTorr, 200 cm/sec; B) 350 mTorr, 100 cm/sec; C) 0.5 W/cm^2, 1.2E-10 moles/cc. R_{sq} = 0.915 for this model fit.

film axial uniformity are given in three contour plots in Fig. 4. The response plotted here is the uniformity factor, R_{av}/R_{max}. Axial uniformity is nearly 1.0 over a broad range of power density and HMDSO concentration in the low pressure (150 mTorr), high gas-velocity (200 cm/sec) region of Fig. 4a. High power at low HMDSO concentration causes non uniformity because of HMDSO depletion along the flow path. At higher pressure (350 mTorr) and lower velocity (100 cm/sec), Fig. 4b shows the onset of non uniformity at moderate power densities. Finally, Fig. 4c shows effects of pressure and gas velocity on uniformity, at 0.5 W/cm^2 and 1.2E-10 moles/cc HMDSO. Generally, uniformity improves with increasing gas velocity and with decreasing pressure. Both of these conditions tend to reduce HMDSO depletion along the electrode surface.

O_2 Permeation Rates - SiO_x Barrier Coatings

Measured O_2TR rates that have been normalized to a 1,000 Å SiO_x film thickness on 2 mil PET are listed in the final column of Table I. The barrier film thickness on the O_2 permeation test samples differed from sample to sample, but was typically in the range of 600 Å to 1,200 Å. Adjustment was made by calculating the O_2 permeability of each SiO_x film based on actual film thickness, then using this permeability to calculate O_2TR for a 1,000 Å thick film. This calculation was based on the two-layer permeation equation:

$$L_s/P_s + L_f/P_f = L_e/P_e = 1/R_e \qquad (1)$$

where L and P are the thickness and permeability, respectively, of the PET substrate (s), the SiO_x film (f), and the effective double layer (e). The effective permeability, P_e (cc mil/m^2 day atm), is derived by multiplying the measured O_2 permeation rate, R_e (cc/m^2 day atm) by thickness L_e.

Examination of the O_2TR data in Table I shows a wide variation in O_2TR from run to run, from 1 cc/m^2 day to 30 cc/m^2 day. The O_2 permeation rate of the uncoated 2 mil PET substrate was about 30 cc/m^2 day. One obvious trend in the Table I data is that most of the low-HMDSO-concentration runs (Runs 1-8) of the factorial portion of the experiment produced relatively good barriers, the exception being Run 4, where film thickness distribution was very non uniform. In contrast, many of the high concentration runs of the factorial (Runs 9-16) produced relatively poor barriers. There was rather large variability in the O_2TR measurements, as is evident in the spread in the centerpoint O_2TR values (Runs 25-30). Good repeatability of O_2TR measurements on individual samples indicated that most of the observed variability resulted from sample preparation effects. Overall, the O_2TR data is intended to indicate general trends only.

Typical contour plots for the polynomial fit to the normalized O_2TR data are given Fig. 5. At the centerpoint conditions of 250 mTorr and 150 cm/sec gas velocity (Fig. 5a), a broad minimum exists, centered at ~ 0.5 W/cm^2 and 1.8 E-10 moles/cc HMDSO. Comparison with Fig. 3a shows that process conditions producing the highest and lowest deposition rates produce poor barrier films. Poor barrier films can result from one or more of three factors: 1) high O_2 permeability of the SiO_x film; 2) poor thickness uniformity, resulting in uncoated areas; and 3) low average thickness / deposition rate.

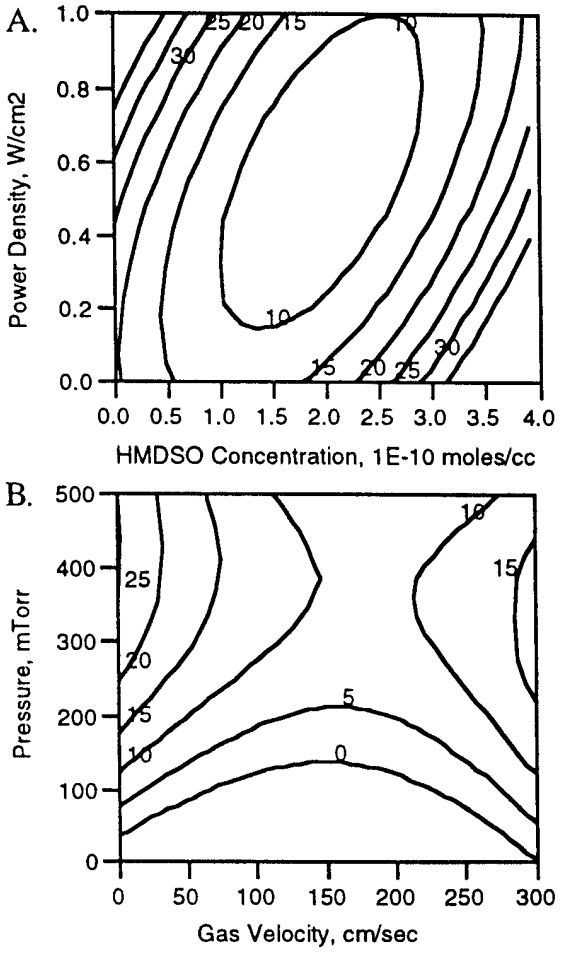

Fig. 5. Behavior of the measured oxygen permeation rate (O_2TR), adjusted for SiO_x film thickness of 1000 Å, as a function of A: HMDSO concentration and power density, with pressure at 250 mTorr and gas velocity set at 150 cm/sec. B: gas velocity and pressure, with HMDSO concentration set at 2.1 E-10 moles/cc, and power density at 0.5 W/cm^2. Both plots are typical of the O_2TR behavior over most of the experimental range studied. R_{sq} = 0.699.

An example of effects of pressure and gas velocity on the normalized O_2 permeation rate is plotted in Fig. 5b, where power density and HMDSO concentration are at the

Table II.	Evaluation of AlOx and AlOx-SiOy Films from TMA and TMA/HMDSO Precursors									
Precursor Conc		GasVel	Pres-	Power	*Witness*	Unfrmty	Dep.	Avg.	Msrd. Thk	Msrd O2
TMA	HMDSO		sure	Density	*Sample*	Factor	Time	Thickness	at 7 cm	Perm Rate
1E-10 moles/cc		cm/sec	mTorr	W/cm2	*ID No.*		sec	Å	Å	cc/ m2 day
6.8	0.0	156	250	0.70	5073 A		30	3657	1470	n/a
5.1	0.0	206	150	0.30	5073 B		30	4740	5890	n/a
5.1	0.0	206	150	0.30	5073 C		30		6008	9.75
5.0	0.0	210	80	0.30	5073 D		60		8436	26.9
5.0	0.0	210	80	0.50	5073 E		60		10950	19.6 (a)
5.0	1.1	210	80	0.50	5073 F		60		10835	26.4 (a)
1.2	0.0	200	150	0.30	5073 G		60		275	2.86
1.2	0.0	200	150	0.15	5073 H		60		155	18.87
3.0	0.0	200	150	0.30	5073 I	0.578	60	7029	3727	b
3.0	0.0	200	150	0.15	5073 J	0.765	60	7782	7725	b
3.0	0.0	200	150	0.70	5073 K	0.391	30	2027	1958	b
3.0	1.2	200	150	0.30	5073 M		60		5166	b
3.0	1.2	200	150	0.15	5073 N		60		8937	b
3.0	1.2	200	150	0.70	5073 O		30		1094	b
Notes:	(a): Foil masked. Tested over 5 cm2 area.									
	(b): Film thickness distribution too nonuniform for meaningful O2TR test over full area.									

centerpoint levels. The better barriers lie in the low pressure region. Low gas velocity produces poor barrier films except at low pressures. This results at least in part from poor uniformity at low velocity.

There is some evidence that HMDSO-rich process conditions, which yielded high deposition rates, produced SiO_x films that did not show the decrease in O_2TR with thickness expected from Eq. 1. An example is Run 16, where samples coated with films ~ 1,000Å and 2,000 Å thick exhibited approximately the same effective permeation rates. Films deposited under relatively rich HMDSO concentrations also showed some evidence of deterioration of barrier effectiveness with aging.

Characteristics of AlO_x and AlO_x - SiO_y Films

Experimental work on AlO_x films made using the TMA precursor was exploratory and informal compared with the work described above. Fourteen runs using the same reactor setup as described above were performed. Run conditions and available data are listed in Table II. To compare TMA deposition behavior with the behavior of HMDSO in the central composite experiment, many of the TMA run conditions fell within the range used in the HMDSO central composite experiment.

In Runs A and B, seven Si witness samples were distributed along the electrode to measure the deposition-rate profile. These profiles are plotted in Fig. 6. The FTIR spectra from such films were similar to those reported by Bourreau, et. al. [9] for PECVD AlO_x films. The spectra contained features attributed to aluminum oxide, hydroxide, and oxy-hydroxide. AlO_x films in Run A were deposited using factor levels near the centerpoint condition of the central composite experiment (250 mTorr, 150 cm/sec), except power density was somewhat higher, and precursor (TMA) concentration was three times higher.

Curve A of Fig. 6 shows that AlO_x deposition rate was very high - above 16,000 Å/min - on the top half of the electrode, then drops off rapidly to near zero. At lower pressure and power density (150 mTorr, 0.30 W/cm^2), curve B shows better uniformity, but deposition rate still drops off rapidly on the bottom half of the electrode. The O_2TR value for this

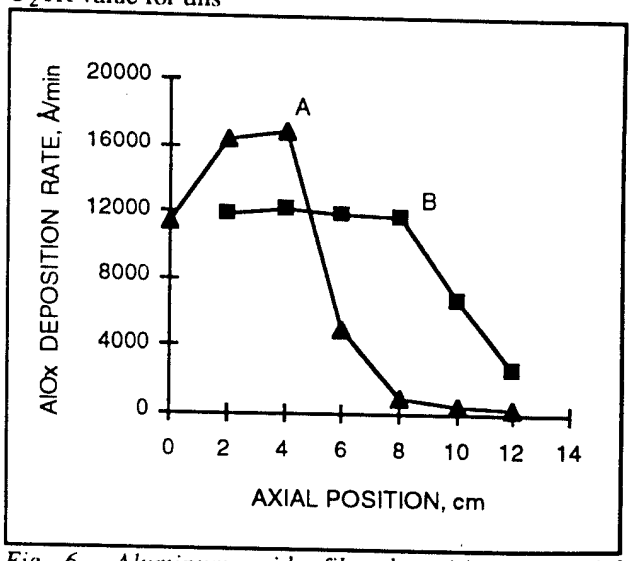

Fig. 6. Aluminum oxide film deposition-rate axial profiles for two different experimental conditions: A) 250 mTorr, 0.5 W/cm^2, 6.8E-10 moles/cc TMA, 156 cm/sec gas velocity. B) 150 mTorr, 0.3 W/cm^2, 5.1E-10 moles/cc TMA, 206 cm/sec gas velocity..

condition (sample C), measured over a 50 cm^2 area, was 9.8 cc/m^2 day (~3x barrier), so this AlO_x was a relatively poor barrier. The non uniform AlO_x film thickness distrib-ution, even under high-deposition-rate conditions, indicates that the TMA reacts much more rapidly on the

electrode than HMDSO does. This correlates with the pyrophoric nature of TMA, whereas HMDSO is stable in air.

Several AlO_x films deposited at low pressure (80 mTorr) to improve uniformity (Runs D, E, and F) contained micro-scopic blisters and cracks. These exhibited high O_2TR values despite their 1 μm thickness. The added HMDSO in Run F did not improve the O_2TR. Runs G through O used parameter settings similar to those in some of the HMDSO central-composite runs. These films were all quite non uniform, therefore full area O_2TR measurements were not performed (except on G and H). For a TMA concentration of 1.2 E-10 mole/cc in Runs G and H, AlO_x deposition rate at mid-plane was less than 300 Å/min. Nevertheless, the O_2TR for G was relatively low, indicating low film O_2 permeability for this case. The uniformity factor calculated for Runs I - K (Table II) was much lower than for SiO_x deposition (from HMDSO) under comparable conditions. Addition of 1.2 E-10 mole/cc HMDSO to the TMA in Runs M-O increased deposition rate, but uniformity remained poor.

CONCLUSIONS

A four-factor designed experiment has shown that the deposition rate and O_2 permeability of SiO_x films deposited from HMDSO precursor vary widely with process parameter settings. The best overall O_2 barrier films were obtained under conditions of low pressure, low HMDSO concentration, and high gas velocity. An exploratory experiment using the precursor TMA has shown that AlO_x films can be deposited at much higher rates than SiO_x from HMDSO. Thickness uniformity was comparatively poor because of the higher reactivity of TMA.

REFERENCES

1. J.T. Felts and A.D. Grubb, "Commercial scale application of plasma processing for polymeric substrates: from laboratory to production", J. Vac. Sci. Technol. A. 10(4) 1675 (1992)
2. J.T. Felts, "Transparent Barrier Coatings Update: Flexible Substrates", Society of Vacuum Coaters, 36th Annual Tech. Conf. Proceedings, 324 (1993)
3. R. W. Phillips, T. Markantes, and C. LeGallee, "Evaporated dielectric colorless films on PET and OPP exhibiting high barriers toward moisture and oxygen", Society of Vacuum Coaters, 36th Annual Tech. Conf. Proceedings, 293 (1993)
4. R.S.A. Kelly, "Development of aluminum oxide clear barrier films", Society of Vacuum Coaters, 37th Annual Tech. Conf. Proceedings, 144 (1994)
5. R.B. Heil, "Mechanical Properties of PECVD Silicon Oxide Based Barrier Films", to be published in proceedings of this conference.
6. G.E.P. Box and N.R. Draper, Empirical Model-Building and Response Surfaces, John Wiley and Sons, New York 1987.
7. JMP Statistical Visualization Software, Vs. 3.0.2, SAS Institute, Inc., Cary, NC
8. J.A. Theil, J.G. Brace, and R.W. Knoll, "Carbon Content of Silicon Oxide Films Deposited by Room Temperature PECVD of HMDSO and Oxygen", J. Vac. Sci. Technol. A12(4), 1365 (1994).
9. C. Bourreau, Y. Catherine, and P. Garcia, "Glow Discharge Deposition of Silicon Oxide and Aluminum Oxide Films: A Kinetic Model of the Surface Processes", Plasma Chemistry and Plasma Processing, 10(2) 247 (1990)

ACKNOWLEDGEMENTS

The authors are grateful to Dr. D. Showers for his encouragemant of this work, and to Mr. A. Kovacich for sharing his expertise in oxygen permeation measurement techniques.